

PROTON NMR IN THE LARGE COMPASS $^{14}\text{NH}_3$ TARGET

J. KOIVUNIEMI*, F. GAUTHERON, C. HESS, YU. KISSELEV, W. MEYER,
E. RADTKE and G. REICHERZ

*Universität Bochum, Institut für Experimentalphysik I,
44780 Bochum, Germany*

**E-mail: Jaakko.Koivuniemi@cern.ch
wwwcompass.cern.ch*

N. DOSHITA, T. IWATA, K. KONDO and T. MICHIGAMI

*Yamagata University, Yamagata,
992-8510 Japan*

In the large COMPASS polarized proton target the 1508 cm^3 of irradiated granular ammonia is polarized with dynamic nuclear polarization method using 4 mm microwaves in 2.5 T field. The nuclear polarization up to 90 - 93 % is determined with cw NMR. The properties of the observed ammonia proton signals are described and spin thermodynamics in high fields is presented. Also the second moment of the NMR line is estimated.

Keywords: polarization, target, proton, ammonia, NMR, DNP

1. Ammonia target

The polarized solid $^{14}\text{NH}_3$ target of the COMPASS experiment at CERN¹⁻³ is using continuous wave NMR to determine the nuclear polarization. During the physics data taking both longitudinal 2.5 T and 1.0 T fields, and transverse 0.63 T field, are used. The homogeneity of the solenoid field is tuned to be better than 20 ppm with the help of 16 trim coils. The Q-meters⁴ are tuned to give the absorption part of the NMR signal. The target proton nuclear polarization is determined with continuous wave NMR. Ten single loop NMR coils 50 mm long and 13 mm wide made from 1.0 mm stainless steel tube are used. Inductance was estimated to be 60 - 80 nH. The coils were mounted on the outer surface of the target cell and connected with 0.9 mm diameter coaxial cable (Precision tube KA50034) inside the mixing chamber to the Q-meters.⁴

The target material is placed into three cells of 4 cm in diameter. The

central cell is 60 cm long and is separated by 5 cm from 30 cm long up- and downstream cells. Each of the cavity volumes can be fed separately with microwaves from outside of the dilution cryostat. Typical ammonia packing factors were 0.46 - 0.52. The solid $^{14}\text{NH}_3$ is polarized through NH_2 radicals.⁵ The natural abundance of deuterons in the protons is 0.0115 % and 0.368 % of nitrogens are nitrogen-15. In addition the volume between the target beads is filled with mixture of helium-3 and helium-4. The target cells are in the diluted phase of the helium mixture, so this is mostly helium-4.⁶ The density of ammonia is about 0.85 g/cm^3 .²

The target cells were made of very thin and light weight materials.⁷ The polyamide mesh had an aramide fiber support structure. Stycast 1266 polymer was used as a glue in the construction. These synthetic fibers and polymers have carbon, hydrogen, nitrogen and oxygen atoms in their molecular structure. A proton background signal can thus be expected in the NMR measurement of the unpolarized signals at temperatures around 1 K. In addition the proton signal could come also from water ice frozen from ambient air during the target filling and loading into the dilution cryostat. The contribution of this proton background was not significant however compared to the cell construction materials.³

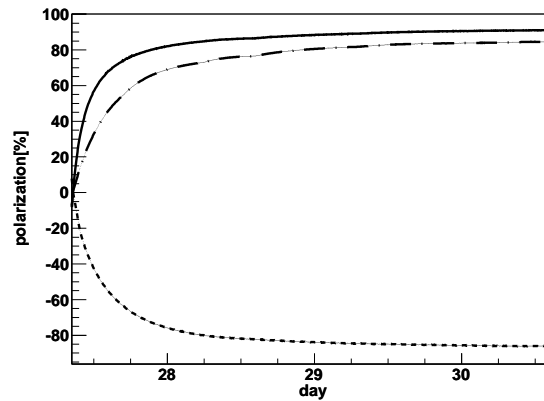


Fig. 1. Typical proton polarization build up. The up- (solid) and downstream (dashed) cells reach +90 % and +85 % polarizations while the central target cell (dotted) is polarized to -87 %. The lower polarization achieved at the downstream cell is probably due to larger microwave guide losses resulting in smaller microwave power compared to the upstream cell. In addition the dilution cryostat cooling is likely not as efficient as at the upstream end of the target, where the helium-3 is circulating more freely.

2. Proton polarization

When the nuclear spin system is in thermal equilibrium with superfluid ^4He the polarization can be calculated from the Brillouin function²

$$P_I(x) = \frac{2I+1}{2I} \coth\left(\frac{2I+1}{2I}x\right) - \frac{1}{2I} \coth\left(\frac{x}{2I}\right), \quad (1)$$

where the spin number $I = \frac{1}{2}$ for protons and $I = 1$ for ^{14}N . Here $x = hf/k_B T_s$ with h the Planck constant, f NMR resonance frequency in 2.5 T field, k_B the Boltzmann constant and T_s the spin temperature. The polarization of the protons at 1.0 K is about 0.25 %. To estimate the statistical error in thermal equilibrium calibration at temperatures 1.0 - 1.5 K a similar data set was produced on computer with the same signal to noise ratio. This was then analyzed with the same programs that were used for the real data. A histogram of the 800 produced calibration constants was fit to a Gaussian to get an error estimate. For the ammonia protons the error was about 1.7 %, while for the background protons it was 5 - 7 % due to the smaller signal. Taking into account the size of the signals these gave an overall statistical error of about 4 % to the final calibration constant after subtraction of the background proton signal. In this simulation the uncertainty comes from the noise and from the temperature measurement.

Typical proton polarization build up is shown in Fig. 1. The helium-3 flow during the polarization was 60 - 70 mmol/s and the temperature in the mixing chamber was 200 - 400 mK. The microwave frequency was about 69 940 MHz for positive polarization and 70 270 MHz for negative. The microwave power is reduced a little at the end of the polarization build up. The frequency modulation of the microwaves has only small about 2 % effect to the final polarization. The average cell polarization was calculated from the three coils on the up- and downstream cells and from the four coils on the central cell.

3. Spin Hamiltonian

For the hydrogen in NH_3 at 2.5 T using cw NMR the nuclear spin Hamiltonian is

$$H = H_z + H_{dip} + H_{quad} + H_{hf} + H_{RF}. \quad (2)$$

In frequency units the Zeeman term is about 106 MHz. The dipolar interaction between two protons at distance of 1.653 Å gives about 25 kHz. The quadrupole term vanishes for the spin $\frac{1}{2}$ while the hyperfine interaction is probably small due to the low density of the paramagnetic centers, about

10^{-4} - 10^{-3} $\text{NH}_2/\text{molecule}$. The continuous wave NMR is usually done at low RF fields, so the last term can also be neglected. Strictly speaking the magnetic field giving rise to the Zeeman term is the local field, which depends on the sample shape.⁸ For a spherical sample the local field is the same as external field however.

The dipole interaction has the simple form^{9,10}

$$D_{zz,jk} = \frac{\mu_0 \hbar \gamma_j \gamma_k}{4\pi r_{j,k}^3} (1 - 3 \cos^2 \theta_{j,k}), \quad (3)$$

where $r_{j,k}$ is the distance between the two nuclei and $\theta_{j,k}$ the angle between the external magnetic field and the position vector between the nuclei. γ_j and γ_k are the gyromagnetic ratios of the two nuclei.

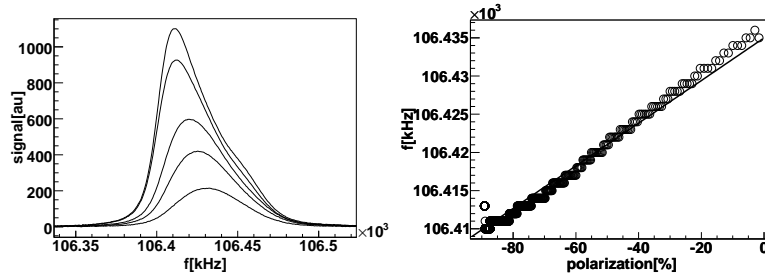


Fig. 2. *Left*: NMR signal line shape for approximate proton polarizations -20 %, -40 %, -60 %, -80 % and -90 %. A memory function fit to the -20 % polarized signal gave $M_2 = 490 \text{ kHz}^2$ and $\mu = 3.7$. At -40 % polarization the fitting of a single line becomes more difficult due to the asymmetry of the lineshape. In this case the $M_2 = 516 \text{ kHz}^2$ and $\mu = 3.9$. *Right*: Typical NMR peak frequency shift during polarization build up. The frequency shift of the peak in coil #4 was fit to a line $106435 + 0.279122 \cdot p$.

The second moment is the sum of the squared frequency shifts from the dipole interaction with neighboring nuclei

$$M_2^j = g_I \sum_k D_{zz,jk}^2 + g_S \sum_l D_{zz,jl}^2. \quad (4)$$

Here g_I is $3I(I+1)/4$ for like spins and g_S is $S(S+1)/3$ for unlike spins.⁹ I is the spin number of the nucleon in consideration and S the spin number of the neighboring unlike nuclei.

For the calculation of the dipolar interaction and the second moment of the proton NMR line the positions of the nitrogen and hydrogen atoms need to be known. Due to the granular nature of the target material, the crystal direction is random in the magnetic field. Here we assume a cubic

lattice with space group $P2_13$.¹¹ The screw axis operation 2_1 rotates the crystal first 180 degree and translates it 1/2 of lattice size along the same axis. In the primitive centering P of the Bravais lattice the points are on the cell corners only. From the initial unit cell positions of one nitrogen atom (x, x, x) , $x = 0.21032$ and one hydrogen atom $(0.3738, 0.2606, 0.1129)$ a lattice is generated applying the symmetry operations in this space group. The lattice constant $a=5.1305$ Å agrees well with the measured density of 0.85 g/cm³. The molecular structure of ammonia is assumed to be preserved with $r_{\text{NH}} = 1.0099$ Å, $r_{\text{NN}} = 3.3769$ Å and H-N-H bond angle of $107.5 - 109.0^\circ$.¹¹

After a sufficiently large lattice has been generated, it is cut into a spherical shape. The dipolar interaction and second moments of the central hydrogens are then calculated. Next the sample is rotated with Euler angles (α, β, γ) to a random direction and the calculation of M_2 is repeated. This is done about 1000 times to simulate the number of crystals seen by each NMR coil. The simulation resulted for this static model a M_2 of about 890 kHz². This is of course larger than in a simple one molecule simulation, since the proton spin sees also all the other neighboring molecules.

4. Proton lineshape

In the solids the NMR linewidth is usually determined by the dipole and quadrupole interactions. In case of spin $\frac{1}{2}$ protons the quadrupole interaction is absent. The indirect coupling gives normally frequency shifts of a fraction of hertz and requires high resolution NMR to be used.¹² It has been suggested that the covalent bond with the nitrogen could mediate the indirect interaction between the protons.² Recently the J-coupling has been observed between two magnetically active nuclei on both sides of a hydrogen bond.¹³ Proton tunneling in the hydrogen bond could also play a role in the lineshape.¹⁴ The classical paper of Van Vleck¹⁵ calculated the second moment of the NMR line. In the dipole interaction the odd moments vanish resulting in a symmetric lineshape and the lineshape is independent of polarization or sample shape. Abragam calculated the polarized case of a spherical sample of one species of nuclear spins coupled by pure dipole interaction and found a good agreement to $M_2(p) = M_2(0)[1 - p^2]$ in case of CaF₂.¹⁶ Here at maximum polarization $p=1$ the second moment goes to zero. While the NMR line can be seen to become narrower due to the polarization build up, it does not seem to follow such a simple law in case of ammonia. The thermal equilibrium signal at 1.0 K from the background protons is shown in Fig. 3. It is clearly wider than the signal from ammonia,

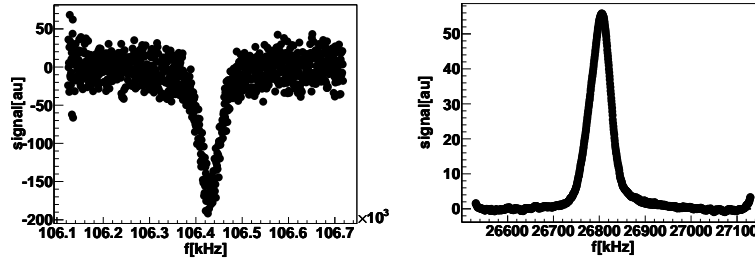


Fig. 3. *Left*: Empty target cell signal at 1.0 K in 2.5 T field from coil #6. From the fit $M_2=1071$ kHz² and $\mu=5.5$. *Right*: Proton NMR signal measured in transverse 0.63 T field with polarization of +82 %. Since the Q-meter is not tuned for this frequency a phase correction of 1.6 rad was done using the Kronig-Kramers dispersion relations. The fit to a memory function gave $M_2 = 815$ kHz² and $\mu=4.5$. The lineshape does not have clear asymmetry like in the much more homogeneous longitudinal 2.5 T field. The reason for this can also be the Q-meter base line subtraction.

where $M_2 = 520 - 650$ kHz² and $\mu = M_4/M_2^2 \sim 3.8 - 4.0$. The integrated intensity of the background protons was about 20 % of the ammonia proton intensity. The +82 % polarized signal in transverse 0.63 T field is also shown. Broader linewidth can be due to less homogeneous magnetic field. The radio frequency field from the detection coil is not orthogonal to the static field in this case.

5. Spin thermodynamics

Nuclear spin entropy^{2,8} in high field taking into account only the Zeeman term of the spin Hamiltonian in Eq. 2 is

$$S_n/R = \frac{x}{2I} \coth \frac{x}{2I} - \frac{(2I+1)x}{2I} \coth \frac{(2I+1)x}{2I} + \ln \left(\frac{\sinh \frac{(2I+1)x}{2I}}{\sinh \frac{x}{2I}} \right). \quad (5)$$

Here R is the universal gas constant. The polarization values of 90 % correspond to spin temperatures around 1.7 mK. The entropy density for the protons reduces to 1.65 J/mol K from the initial unpolarized 5.76 J/mol K. If the conditions for dynamic nuclear polarization are assumed to be the same for all of the coils on each target cell, the variations in the final polarization values could reflect small differences in the polarizable spin density along each cell.

Table 1. Typical maximum polarizations probed by the NMR coils. The NMR peak position is determined by the magnetic field homogeneity and the target polarization. Also the calculated spin temperature, entropy and nuclear heat capacity are given.

Coil	p [%]	f [kHz]	T_n [mK]	S_n [J/mol K]	C_B [J/mol K]
1	+90.4	106459	+1.7	1.6	3.4
2	+90.3	106462	+1.7	1.6	3.4
3	+92.5	106463	+1.6	1.3	3.2
4	-89.1	106413	-1.8	1.8	3.5
5	-87.2	106408	-1.9	2.0	3.6
6	-86.8	106406	-1.9	2.0	3.6
7	-83.7	106408	-2.2	2.4	3.7
8	+82.9	106453	+2.2	2.4	3.7
9	+77.2	106456	+2.5	2.9	3.5
10	+93.5	106449	+1.5	1.2	3.0

One of the interesting properties of water ice at low temperatures is its residual entropy.¹⁷ As pointed out by Pauling in his paper the hydrogen bonds do not always lead to residual entropy. It is however interesting to estimate upper limit for this in case of ammonia ice. In similar way like in the Pauling's calculation, the "ammonia rules" require that each nitrogen has three close hydrogen neighbors to preserve the molecule structure. In addition the nitrogen has three distant hydrogens that reside close to other three nitrogens. For N nitrogens and $3N$ hydrogens the total number of configurations is then 2^{3N} . For the six hydrogens on each of the nitrogen atoms there are $2^6 = 64$ possible combinations. From these only 20 full fill the "ammonia rules". Thus upper limit for entropy

$$S_0 = k_B \ln \left(2^{3N} \left(\frac{20}{64} \right)^N \right) = N k_B \ln \left(\frac{5}{2} \right) \quad (6)$$

gives 7.6 J/mol K compared to the 3.4 J/mol K in the water ice.

The nuclear heat capacity in constant external magnetic field $C_B = T(\partial S_n / \partial T)_B$ becomes

$$C_B/R = \frac{x^2}{(2I)^2} \frac{1}{\sinh^2 \frac{x}{2I}} - \frac{(2I+1)^2 x^2}{(2I)^2} \frac{1}{\sinh^2 \frac{(2I+1)x}{2I}}. \quad (7)$$

Thus the 90 % polarized proton nuclear heat capacity in 2.5 T field is then about 3.4 J/mol K while at zero polarization the heat capacity goes to zero. This is the reason why the relaxation of the polarization in the "frozen spin targets" is very slow at low temperatures. The Eq. 7 relates the heat flow to the spin system to the polarization relaxation rate. For

example polarization loss in one day from 90 % to 89 % corresponds to a heat flow of about 2 nW/mol in 2.5 T field at temperatures below 60 mK.

References

1. P. Abbon et al., *Nucl. Instr. Meth.* **A577**, 455–518 (2007).
2. B. Adeva et al., *Nucl. Instr. Meth.* **A419**, 60–82 (1998).
3. J. Koivuniemi et al., *Journal of Physics: Conference Series* **150**, 012023 (2009).
4. K. Kondo et al., *Nucl. Instr. Meth.* **A526**, 70–75 (2004).
5. W. Meyer, *Nucl. Instr. and Meth.* **A526**, 12–21 (2004).
6. N. Doshita et al., *Nucl. Instr. Meth.* **A526**, 138–143 (2004).
7. S. Neliba et al., *Nucl. Instr. Meth.* **A526**, 144–146 (2004).
8. O. V. Lounasmaa, *Experimental Principles and Methods Below 1 K*, Academic Press, London (1974).
9. A. Abragam, *The Principles of Nuclear Magnetism*, Oxford University Press, Hong-Kong (1989).
10. M. Mehring, *Principles of High Resolution NMR in Solids*, Springer-Verlag, Heidelberg (1983).
11. R. Boese et al., *J. Phys. Chem.* **101**, 5794–5799 (1997).
12. N. F. Ramsey, *Phys. Rev.* **91**, 303–307 (1953).
13. A. J. Dingley, F. Cordier, S. Grzesiek, *Concepts in Magnetic Resonance* **13(2)**, 103–127 (2001).
14. A. J. Horsewill and W. Wu, *J. Magn. Reson.* **179**, 169–172 (2006).
15. J. H. Van Vleck, *Phys. Rev.* **74**, 1168–1183 (1948).
16. A. Abragam et al., *J. Magn. Reson.* **10**, 322–346 (1973).
17. L. Pauling, *J. Am. Chem. Soc.* **57**, 2680–2684 (1935).